Simulation

Applications

Simulation: Transactions of the Society for Modeling and Simulation International
1–14

DOI: 10.1177/0037549718788955
journals.sagepub.com/home/sim
SAGE SCS

Simulation of time series wind speed at an international airport

Ronald Wesonga[1,3], Fabian Nabugoomu[2], Faisal Ababneh[3,4] and Abraham Owino[1]

Abstract

The sporadic and unstable nature of wind speed renders it very difficult to predict accurately to serve various decisions, such as safety in the air traffic flow and reliable power generation system. In this study we assessed the autoregressive integrated moving average (ARIMA) and artificial neural network (ANN) models on the wind speed time series problem. Data on wind speed and minimum and maximum temperatures were evaluated. Wind speed was established to follow a time series that fluctuated around ARIMA (0,1,1) and ARIMA (1,1,1). The optimal ANN model was established at 10 hidden neurons. The performance indices considered all indicated that the ANN wind speed model was superior to the ARIMA model. Wind speed prediction accuracy can be improved to secure the safety of air traffic flow as well support the implementation of a reliable and secure power generation system at the airport.

Keywords

Wind speed, autoregressive integrated moving average, artificial neural network, model, statistics

1. Introduction

The sporadic and unstable nature of wind speed renders it very difficult to predict accurately. Scarcity of information and related studies about wind speed at Entebbe International Airport is another key factor hindering sustainable development at the airport. Accurate wind speed forecasting would play a vital role in securing the safety mandate of the Air Traffic Flow Management at the airport. The forecasting information is as well crucial to the reliable and secure power generation system, especially at airports in the developing countries. The lack of such information could be the main reason why the airport suffers from inept air traffic flow management as well as delayed implementation of clean energy projects.

In statistics, many types of models are developed to inform decisions in various disciplines, including the environment. However, the general guidelines are often faced with limitations in so far as they apply, thus requiring further model investigation. In stochastic time series analysis, models such as autoregressive integrated moving average (ARIMA) and artificial neural networks (ANNs) have been developed and are used to make predictions. Often times, information criteria, such as the AIC (Akaike Information Criterion) and the BIC (Bayesian Information Criterion), are used to compare and select better models for use in specific circumstances.[1] In this study, we evaluated the two stochastic models to predict wind speed. The ANN models[2–4] and the ARIMA models[5,6] are described in the subsequent sections. As an application, the maximum wind speed values for Entebbe International Airport were modeled. In addition, wind speed prediction errors for the two derived models were analyzed to further ascertain the reliability of the prediction models.[7,8]

The vicinity of Entebbe International Airport to a lake renders it vulnerable to the dynamic weather phenomenon caused by frequent changes in wind speed, wind components, and evaporation at Lake Victoria.[9] Usually, winds of thermal origin blow from the lake during the day and land winds occur at night. The onshore–offshore air temperature gradient during the day is highest, and winds are generally strongest, in the dry season. High evaporation experienced at the lake is associated with south winds because wind speed at the lake is generally highest from the south, partly

[1]School of Statistics and Planning, Makerere University, Uganda
[2]Kyambogo University, Uganda
[3]Sultan Qaboos University, Oman
[4]Al-Hussein Bin Talal University Maan, Jordan

Corresponding author:
Ronald Wesonga, Department of Mathematics and Statistics, Sultan Qaboos University, PO Box 36, Al Khoud 123, Sultanate of Oman.
Email: wesonga@wesonga.com

due to the southeast trade winds during the dry season. Evaporation of the lake is influenced by the pattern of land and lake winds.[10] The winds at this airport are a source of various weather patterns experienced at different times of the day, including rainfall and visibility, a major parameter that concerns air traffic flow management.

Data on wind speed recorded at Entebbe International Airport were used to generate wind speed prevalence and also test the models for their predictive efficacies. Wind speed data explorations at a 10-day frequency over a relatively long period of time were made to comprehend the stable dynamics of wind speed over time. The study is unique because other studies[11,12] did not explore such methodologies, making this study the first to present stochastic models while performing a comparative analysis of decadal wind speed data at an international airport. This study makes a contribution toward understanding the efficacies of ARIMA and ANN models in time series analysis and the general knowledge of the wind speed phenomenon.[13,14] The case of decadal wind speed data modeling, like all other time series data analysis, provides precursors of scenarios to planners and implementers of projects that depend on wind, such as the requirement for wind energy turbine repairs and maintenance activities. Furthermore, wind energy generation, although known to require high wind speeds at relatively smaller regular frequencies, requires relatively longer periods to be studied for the environment with which it interfaces, and hence an optimal data frequency of a 10-day wind speed analysis and modeling was preferred.

2. Materials and methods

2.1 Data

Daily aggregates of wind speed data were collected over the period 1995–2008, generating a data matrix of 168 months, three decadal maximum wind speed measured in miles per second. The data were reconstructed and classified according to the decadal in which they fell and, for each decadal, the value of maximum wind speeds was identified. In this study, a decadal refers to the measurement of wind speed within a period of 10 days. On average, there are 30 days in a month, generating three decadal data points in every month. Further description of the data can be found in the work on multivariate imputations of wind speed data.[15] The dataset is archived by Figshare, a repository for research outputs, and accessible at the uniform resource locator 10.6084/m9.figshare.3804357.

Data reconstruction considered only maximum wind speeds that were cogitated to be meaningfully relevant in agitating for the wind energy generation project. We assume $Y_{1995} \ldots Y_{2008}$ to be the years under study, $M_1 \ldots M_{12}$ to represent months within a year, and $D_1 \ldots D_{31}$ a sample space for days in a month. Possible three decadal wind speed data are thus $\{D_{101\rightarrow110}, D_{211\rightarrow220}, D_{321\rightarrow331}\}$. For each decadal, a maximum value was determined, thus obtaining aggregated three maximum wind decadal values within a given month as $\{mWD_1, mWD_2, mWD_3\}$ obtained from$\{\max W(D_{101\rightarrow110}), \max\ W(D_{111\rightarrow120}), \max W(D_{121\rightarrow131})\}$. The data structure for the variable containing reconstructed maximum wind speed values was of the order such that for a given year and month, the maximum wind values for decadal one were listed, then decadals two and three, respectively.

ANNs and the ARIMAs are known to assume inherent self-prediction. However, from the theoretical underpinnings, wind speed is determined by temperature gradients between two areas. Excitation of air particles ignites the takeoff velocities of air molecules that subsequently move at various speeds from high-temperature to low-temperature areas, hence consideration of temperature. All algorithms, modeling, and development in this study were done using R statistical programming and MATLAB. Specifically, the following R packages have been used in the ARIMA and ANN model development and analysis; library (''TTR''), library (''forecast''), library (''neuralnet''), and library (''nnet'').[16,17]

2.2 Autoregressive integrated moving average

We fit a time series model because of the nature of historic wind speed data used so as to investigate and predict wind speed series spaced at regular intervals of time. The ARIMA model approach is important for studying the statistical structure of data.[18] The approach also investigates trends; seasonal patterns and periods; cycles; and the irregular statistical fluctuations about overall wind speed mean or trend.[17,19] The general expression for the ARIMA (p, d, q) model can be written as follows:

$$X_t = c + \omega_1 X_{t-1} + \ldots + \omega_p X_{t-p} + \theta_1 e_{t-1} + \ldots + \theta_q e_{t-q} + e_t \quad (1)$$

where $\omega_1, \omega_2 \ldots \omega_p$ are autoregressive parameters and $X_t, X_{t-1} \ldots X_{t-p}$ are measured values at $t, t-1, t-2 \ldots t-p$, respectively; and α_t is the uncorrelated error found to be normally distributed with mean zero $[\sim N(\mu = 0, \sigma = 1)]$. The equation represents both the non-seasonal and seasonal parts of the model. The ARIMA model was used to predict the mean values of wind speed, and the predictions were compared with those obtained from multilayer feed-forward ANNs.[17] The autocorrelation function characterizes the pattern of wind speed persistence. The sample autocorrelation coefficients were obtained using the following:

$$r_k = \frac{\sum_{t=1}^{n-k}(X_t - \bar{X})(X_{k+t} - \bar{X})}{\sum_{t=1}^{n}(X_t - \bar{X})^2} \quad (2)$$

where r_k is the sample autocorrelation coefficient, k is the time lag, $\bar{X}$ is the mean decadal wind speed, and n is the total number of training data.[17] The mean decadal wind speed $\bar{X}$ was calculated from the following:

$$\bar{X} = \frac{\sum_{t=1}^{n} X_t}{n} \tag{3}$$

The autocorrelation function gives an indication about the order of differencing for the model and can also be used to best fit the wind speed data.

2.3 Artificial neural networks

ANNs have been developed to mimic natural intelligence from human beings.[20–23] They learn from examples by constructing an input–output mapping without explicit derivation of the model equation. Some of the prediction advantages identified include their ability to do the following: (1) offer computationally intelligent prediction systems; (2) present model free dynamics to predictions; (3) be referred to as universal approximates because they offer a larger number of classes of functions, a high degree of accuracy, and incredibly generate reliable information from data; (4) require no prior assumptions of the model form in the model building process; and (5) use a network model that is largely determined from the characteristics of the data. ANNs have been applied broadly in fields such as pattern classification, function approximation, optimization, prediction, and automatic control, among others. An ANN consists of many interconnected identical simple processing units called neurons.[3,23–25] Each connection to a neuron has an adjustable weight factor associated with it. Therefore, an internal activity level V_i is obtained when every neuron in the network sums its weighted inputs:

$$V_i = \sum_{j=1}^{n} W_{ij} X_{ij} - W_{i0} \tag{4}$$

Variables in Equation (4) are described as follows: W_{ij} – the weight of the connection from input j to neuron i; X_{ij} – the input signal number j to neuron i; and W_{i0}– the threshold associated with unit i. Here, the threshold is treated as a normal weight with the input clamped at -1, whereas the internal activity is dispatched through a nonlinear function $\varphi()$ to produce the output of neuron Y_i:

$$Y_i = \varphi(V_i) \tag{5}$$

To achieve the desired input–output relation of the network, weights of the connections are adjusted during the training process. Artificial networks come in many different paradigms, some require topologies with total interconnection among neurons and others require arrangements in layers.[26–28] A multilayer feed-forward network has its neurons organized into layers with no feedback or lateral connections. Layers of neurons other than the output layers are referred to as hidden layers. Whereas the input signal propagates through the network in a forward direction, on a layer-by-layer basis, the back-propagation algorithm is a supervised iterative training method for multilayer feed-forward networks with sigmoidal nonlinear threshold units that uses training data consisting of p input–output pairs of vectors that characterize the problem.[29]

The generalized least square algorithm can be used by the back-propagation algorithm to minimize the mean square difference between the real network output and the desired output. Thus, the error function that the back-propagation algorithm minimizes is the average of the squared difference between the output of each neuron in the output layer and the desired output.[2,23] The error function is thus expressed as follows:

$$E = \frac{\sum_p \sum_k \left(D_{pk} - O_{pk}\right)^2}{2P} \tag{6}$$

where p is the index of the P training pair of vectors, k is the index of elements in the output vector, D_{pk} is the kth element of the pth desired pattern vector, and O_{pk} is the kth element of the output vector when pattern p is presented as input to the network.

The error function E can be minimized, resulting in an updating rule that adjusts the weights of the connections between neurons. The weight adjustment of the connection between neuron i in layer j in layer $m + 1$ is expressed as follows:

$$\Delta W_{ji} = \eta \delta_j O_i \tag{7}$$

where i is the index of units in layer m, η is the learning rate, O_i is the output of unit i in the mth layer, and δ_j is the delta error term back-propagated from the jth unit in layer $m + 1$ and is defined by the following:

$$\delta_j = \begin{cases} \left[D_j - O_j\right] O_j \left[1 - O_j\right]; \text{if neuron } j \text{ is in the output layer} \\ Y_j \left[1 - Y_j\right] \sum_k \delta_k W_{kj}; \text{ if neuron } j \text{ is in a hidden layer} \end{cases} \tag{8}$$

where k is the index of neurons in the layer $(m + 2)$, ahead of layer of neuron j. Thus, a small learning rate η leads to a slow rate of convergence, while a large η leads to oscillation.[23] To increase the rate of learning without oscillation, a momentum term is included:

$$\Delta W_{ji}(n + 1) = \eta \delta_j O_i + \alpha \Delta W_{ji}(n) \tag{9}$$

where n is the iteration number and α is a positive constant that determines the effect of past weight changes on the current direction of movement in weight space. Therefore, the application of the ANNs to wind time series prediction takes the format as follows:

Table 1. Summary statistics of wind speed and minimum and maximum temperature (1995–2008).

Descriptive statistics	Wind speed (m/s)	Minimum temperature (degree Celsius)	Maximum temperature (degree Celsius)
Number of decadals	504	504	504
Minimum	9.00	14.90	22.06
Maximum	48.00	20.56	31.04
Mean	17.52	18.55	26.33
P25	14.00	18.06	25.55
P50	15.50	18.54	26.15
P75	20.00	18.98	27.00
Standard deviation	5.49	0.70	1.26
Standard error of the mean	0.24	0.03	0.06
Skewness	1.79	− 0.03	0.54
Kurtosis	7.76	4.01	4.70

$$Y_t = W_0 + \sum_{j=1}^{q} W_j g(W_{0j} + \sum_{i=1}^{p} W_{ij} Y_{t-i}) + \varepsilon_t \qquad (10)$$

W_{ij} and W_j are model parameters (often called connection weights), $p$are inputs of wind speed, and q are hidden nodes. Activation functions are required more for the output layer than the input layer. The main role of the input layer neurons is to transfer inputs to the hidden layer, hence they do not have the activation function.[30] We note that the most widely used functions for the output layer are the linear functions, since nonlinear functions would introduce distortions to the produced output.[23] Often times, the following logistic functions are used as hidden layer transfer functions. Logistic function of the following form:

$$sig(X) = \frac{1}{(1 + \exp(-X))} \qquad (11)$$

and the hyperbolic function of the following form:

$$\tanh(X) = \frac{(1 - \exp(-2X))}{(1 + \exp(-2X))} \qquad (12)$$

We notice that $Y_t = f\left(Y_{t-1}, Y_{t-2} \ldots Y_{t-p}, W\right) + \varepsilon_t$, where W is a vector of all parameters and $f(.)$ is determined by the structure and connection weights of the neural network resulting in a nonlinear $AR(p)$.[23,31–33]

3. Results

3.1 Descriptive analysis

We compare results from the ARIMA and ANN models to be able to identify a better model framework for statistical analysis. Table 1 shows that the average wind speed at Entebbe international airport is 17.52 ± 0.48 m/s. The wind speed has a positive skewness and flunctuates between a minimum of 9 and 48 m/s. It should be noted that windspeed, unlike minimum and maximum temperature data, had missingness completely at random. The study employed the multivariate imputation method to impute the missing data using MICE (multiple imputations by chained equations), an R package based on the Markov Chain Monte Carlo (MCMC) framework.[15]

Further, Figure 1 shows the time series plot of the decadal wind speed for the period 1995–2008.

3.2 ARIMA model for wind speeds

ARIMA models for wind speed were derived using the R statistical programming packages that constituted an explicit statistical model for the irregular component of a time series with an allowance for non-zero autocorrelations in the irregular component. The modeling is defined for stationary time series. Thus, if one started off with a non-stationary time series, the time series would require first to be ''differenced'' until a stationary time series is obtained. If the time series is differenced d times to obtain a stationary series, then an ARIMA (p, d, q) model would be determined, where d is the order of differencing used and p and q are orders of auto-regression and moving averages (MAs), respectively. Figure 2 shows the decadal wind speed differenced three times.

The time series of first differences appeared to be more stationary in mean and variance, as the level and variance of the series appeared roughly constant over time. To confirm the order of differencing, we attempted to difference the time series twice and thrice, with no significant difference from the wind time series differenced once (Figure 2). Thus, given that we needed to difference the original wind speed time series data $d = 1$ times in order to obtain a stationary time series, it was implied that the initial model for the wind speed was ARIMA (p, 1, q), where $d = 1$ order of differencing. By taking the time series of first differences, we removed the trend component of the time series of the decadal wind speed, and were left with an irregular component. We then examined whether there were correlations between successive terms

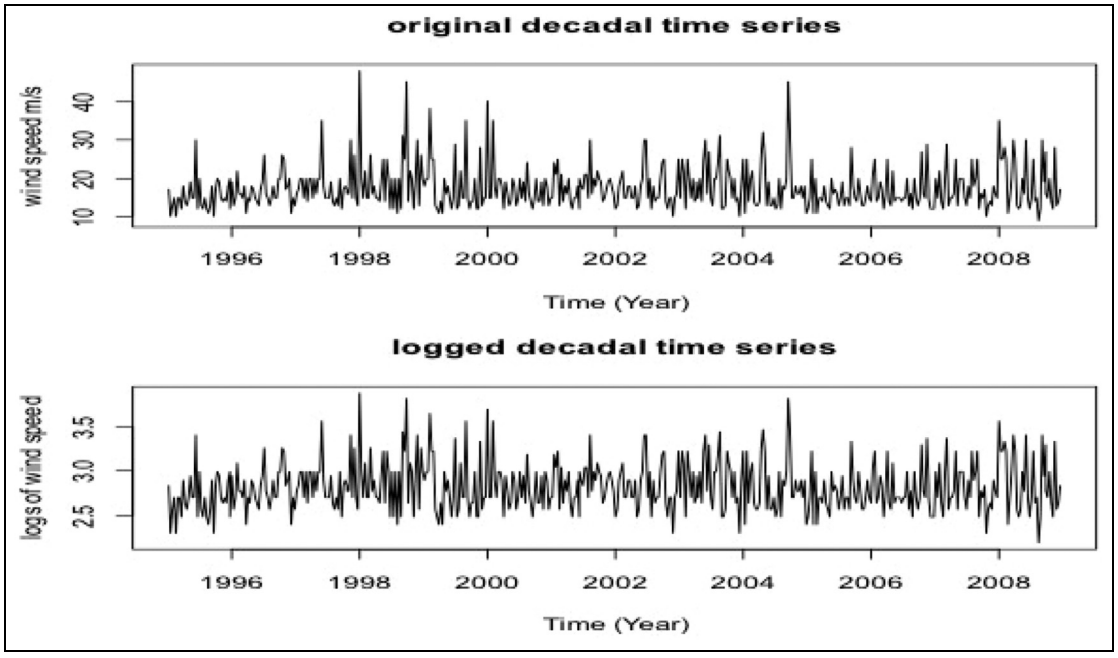

Figure 1. Decadal wind time series.

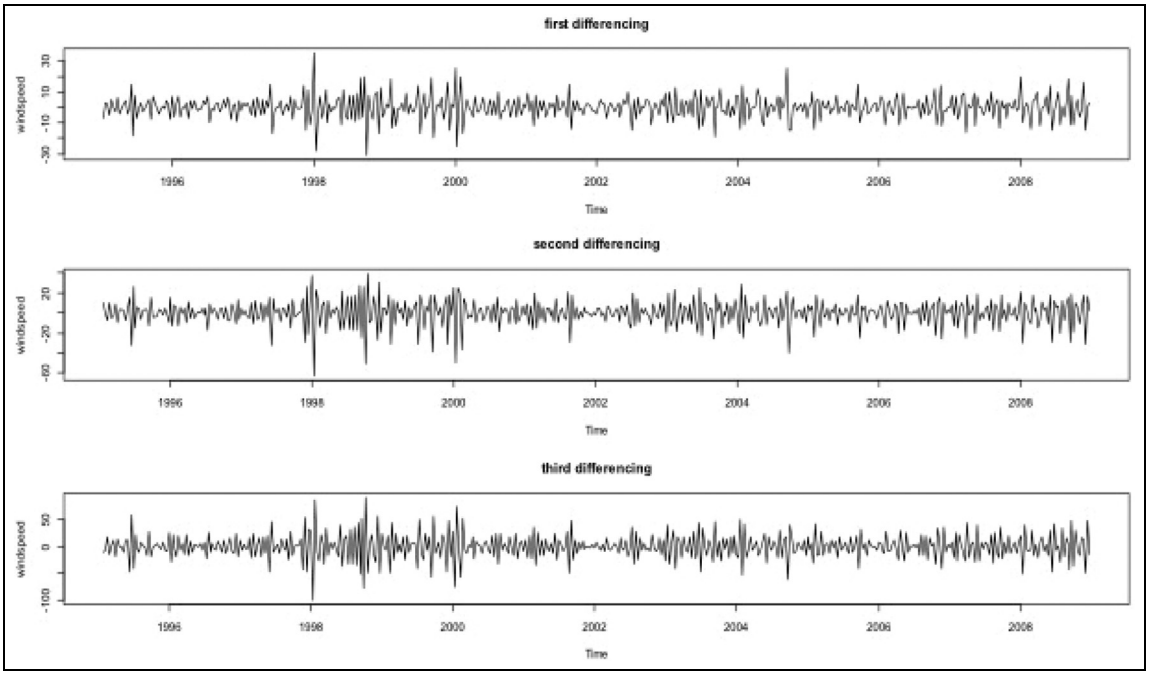

Figure 2. Differenced wind time series at the first, second, and third levels.

of this irregular component; if so, this could have helped us to make a predictive model for the wind speeds.

To find the most appropriate values of p and q for an ARIMA (p, 1, q) model, we then examined the correlogram and partial correlogram of the stationary decadal wind speed time series, as shown in Figure 3.

The best ARIMA model was identified by the elimination method based on the statistical tests including, among others, those listed in Table 2.

After performing different evaluations of the models for ARIMA (p, d, q), the ARIMA (0, 1, 1) model (with p = 0, d = 1, q = 1) was found to be the best model fit for

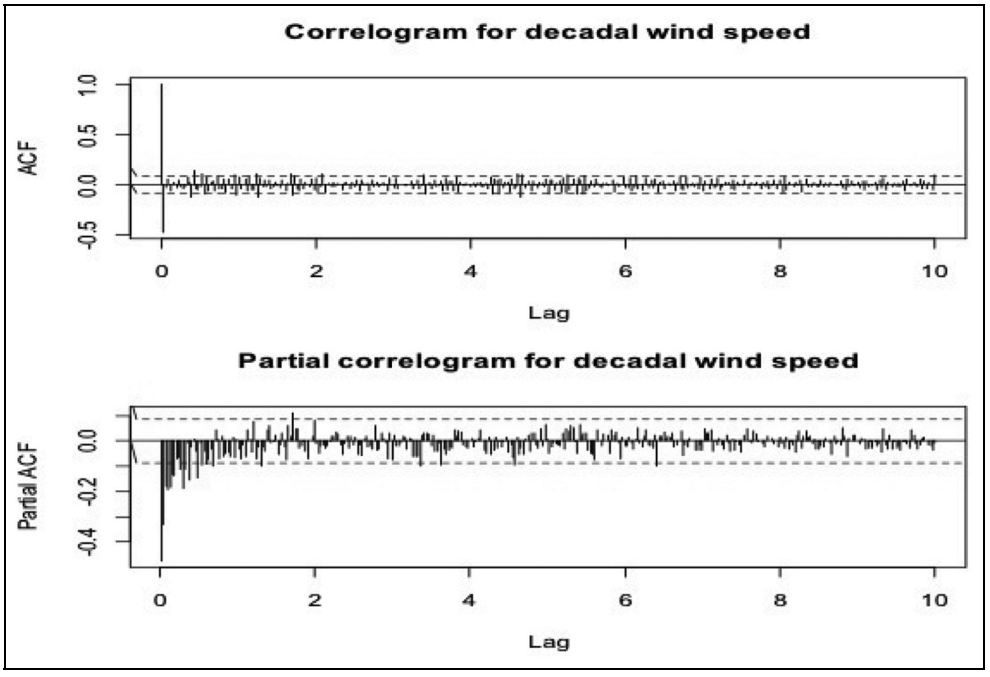

Figure 3. Auto-correlograms and partial correlograms for wind speed. ACF: Autocorrelation function.

Table 2. Efficacy of the autoregressive integrated moving average (ARIMA) model for wind speed.

ARIMA (*p, d, q*)	Variance	Log-likelihood	AIC	*p*-value
ARIMA (1,1,1)	56.22	− 1773.16	3451.18	2.2E-16
ARIMA (0,1,1)	55.42	− 1723.18	3450.36	2.2E-16
ARIMA (1,1,0)	94.40	− 1854.01	3712.02	2.2E-16

AIC: Akaike Information Criterion.

the wind speed time series (Table 2). The value $d = 1$, implies a non-stationary process; the level changes in time, but the increase is constant. Thus, the level is non-stationary, but its increments are. An ARIMA (0, 1, 1) model was derived and takes the estimation form shown as follows:

$$\begin{aligned} \hat{Y}_t - \mu &= Y_{t-1} - \theta\varepsilon_{t-1} \\ \hat{Y}_t &= \mu + Y_{t-1} - \theta\varepsilon_{t-1} \end{aligned} \tag{13}$$

Estimates from the wind speed data revealed a coefficient of the MA1 component to be -0.9751 with a standard error of 0.0127. The other measures of the fitted model were $\chi^2 = 30.27; LL = 1572.89; AIC = 3149.78;$ $BIC = 3158.22$, all of which showed that the fitted ARIMA model was the best given the wind speed in the case study. Error measures too were examined with the following results root mean square error (RMSE) = 5.496; mean absolute error (MAE) = 4.039; mean absolute percentage error (MAPE) = 22.903.

The fitted ARIMA (0, 1, 1) model with a constant is often referred to as simple exponential smoothing (SES) with growth. Implementing the SES model as ARIMA permits some flexibility, since the MA(1) coefficient is allowed to be negative. Thus, when corresponding to a smoothing factor larger than one in a SES model, which the SES model fitting procedure may not allow, one has the option of including a constant term in the ARIMA model as with our case, so as to estimate an average non-zero trend. Fitting the wind speed model, the results are as follows:

$$\hat{Y}_t = 17.524 + Y_{t-1} - 0.975\varepsilon_{t-1} \tag{14}$$

Figure 4 shows graphical analyses of the standardized residuals. The autocorrelation function of the residuals and the *p*-values of a Portmanteau test for the lags all show that the derived ARIMA (0, 1, 1) model is the best model for wind speed. All *p*-values are closer to unity. The correlogram shows that a negligible number of sample autocorrelations for lags 1–10 exceed the significance bounds and the *p*-value for the Ljung–Box test is 0.003. Thus, we

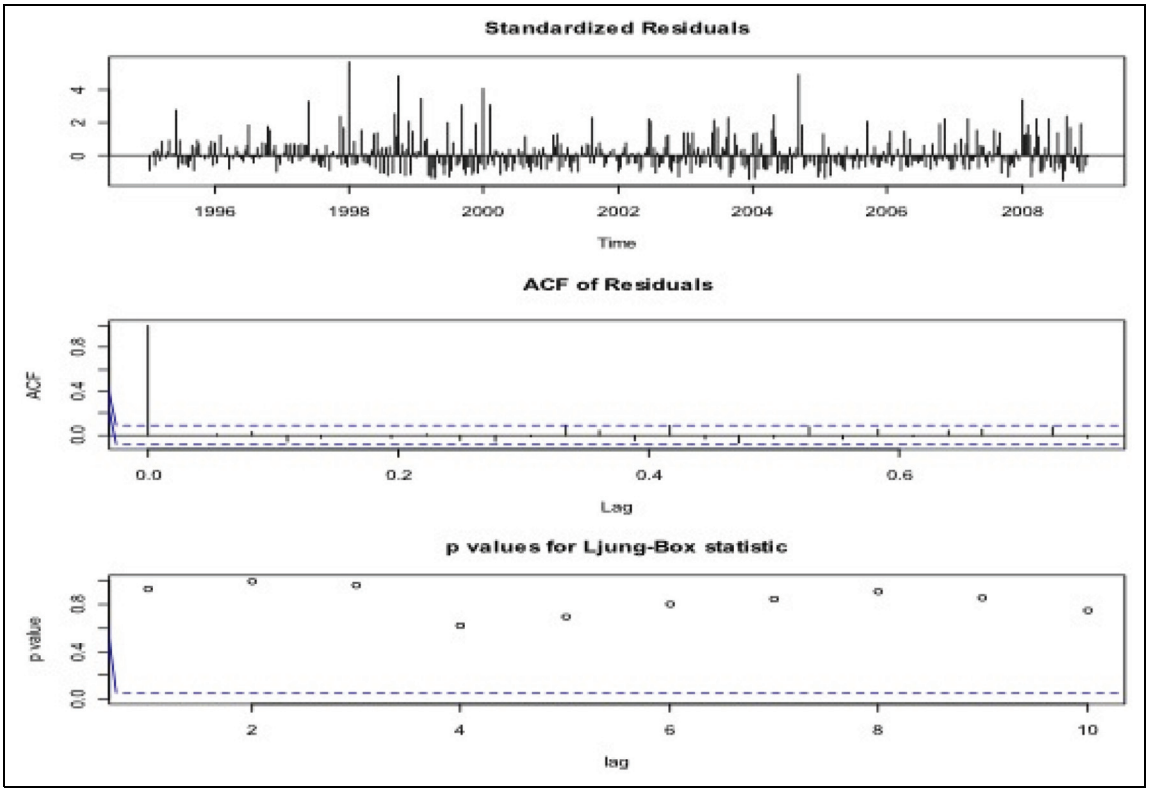

Figure 4. Plot of standardized residuals, their ACFs, and the *p*-values for Ljung–Box statistics. ACF: Autocorrelation function.

conclude that there is little evidence for non-zero autocorrelations in the forecast errors at lags 1–10.

Subsequently, a plot of the original wind speed time series for the period 1995–2008 with predicted wind speed values for the period 2009–2018 was done on the same graph. Visual inspection, besides the earlier technical evidence, shows a good level of efficacy of the wind speed prediction model developed. Figure 5 shows a prediction with 95% confidence bounds for the point estimates of wind speed.

To ascertain the accuracy of the ARIMA model, we checked whether the forecast errors were normally distributed with mean zero and constant variance, by a graphical analysis of a time plot for the forecast errors and a histogram, as shown in the Figure 6. The plots confirm that forecast errors are approximately normally distributed with zero mean and constant variance.

3.3 Artificial neural network model for decadal wind speed

Simulations were performed on a number of data samples to achieve the most suitable ANN[34] that models maximum decadal wind speed. Firstly, determination of covariates yielded the following variables: maximum temperature; minimum temperature; lags for maximum temperature; lags for minimum temperature; and that for the maximum decadal wind speed. Theoretical conception underpinned temperature as the main driver of winds and, statistically, the lag of wind speed itself as a force in enhancing wind speed, as evidenced under ARIMA. A 10% sample of the data was used to train the neural network using a feed-forward perceptron with the back propagation and, subsequently, the neural network was used to predict wind speed. Back propagation is known to use a gradient descent approach to minimize output error in a feed-forward network.[35] Thus, the algorithm presented an input vector, compared the network output to the desired output for that vector, and updated each weight by an amount corresponding to the derivative of the error with respect to that weight times a learning rate, and adjusted by a ''momentum'' factor.

Figure 7 shows five inputs consisting of the covariates described earlier, five neurons in the hidden layer plus one activation function that creates the inevitable bias within the model to output predicted maximum wind speed. In the neural network, the numbers show weights attached to each movement from one node to another. Initially, all of the weights are set to some small random values near zero. The network training adjusts these weights using the back-propagation algorithm so that the output generated by the network matches the correct output.

Figure 8 presents the best evaluated ANN model with AIC and BIC of 72.0054 and 224.0181, respectively, and

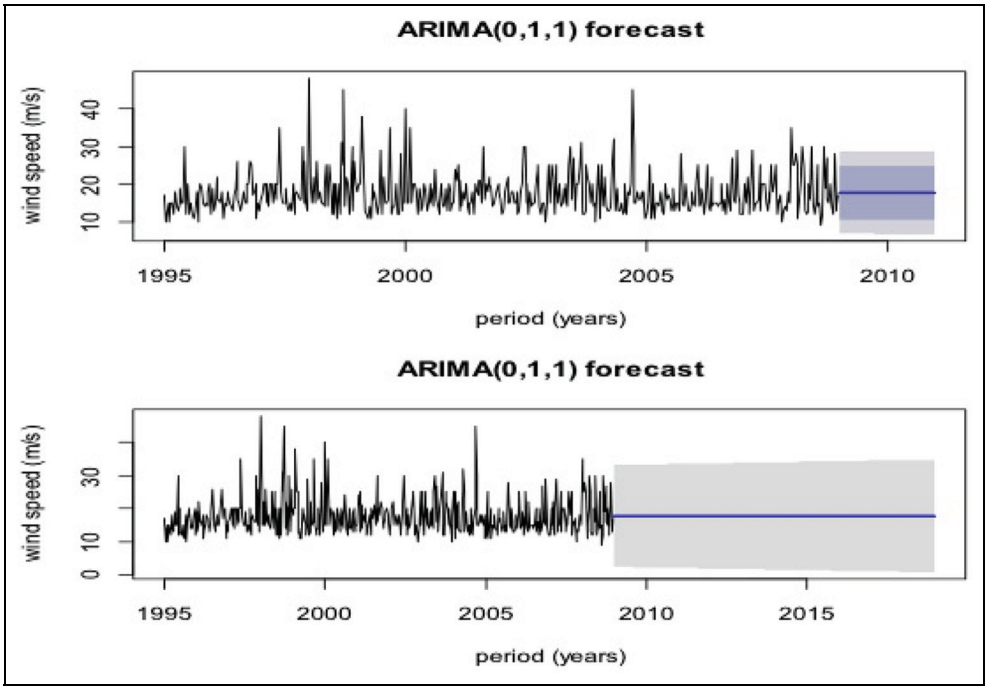

Figure 5. Plot of the autoregressive integrated moving average (ARIMA), predictions at short and long term for the wind speed time series.

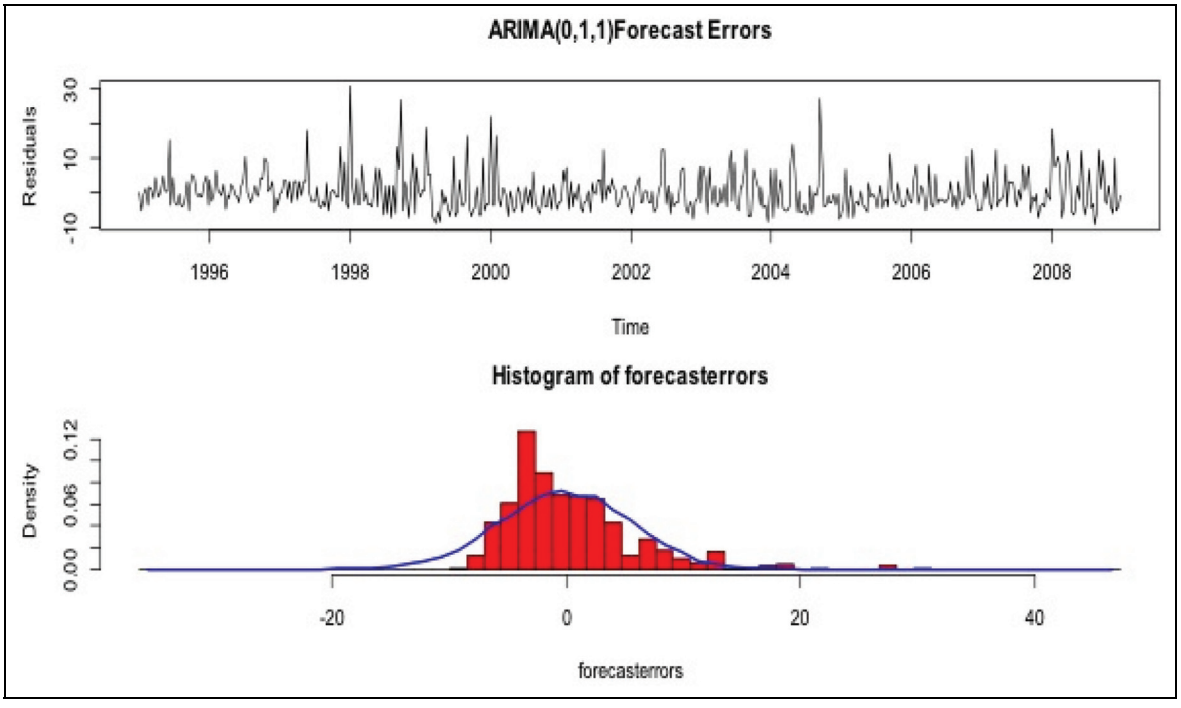

Figure 6. Plot of autoregressive integrated moving average (ARIMA) forecast residual time series and histogram for the residual distributions.

an error of 0.0024, achieved after 54,771 iterative steps, which were attained after about 58 seconds on an Intel Core i5 processor computer. Comparison between the two neural networks shows that the architecture of the ANN in the second figure yields relatively smaller error values and their AIC and BIC are smaller. Its prediction power was

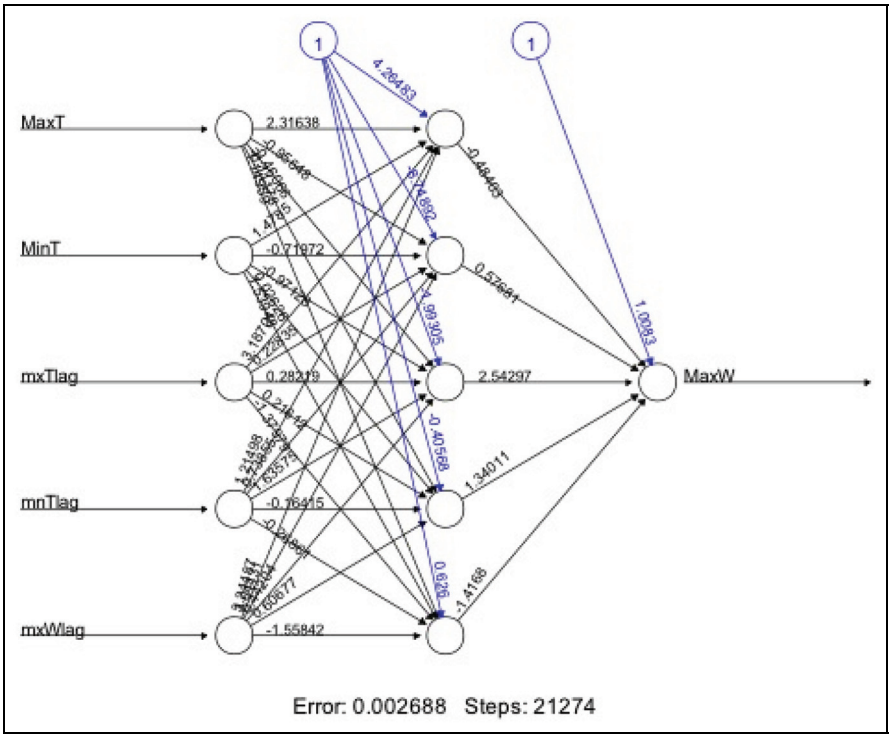

Figure 7. Plot of the artificial neural network showing five neurons in one hidden layer with input and output layers.

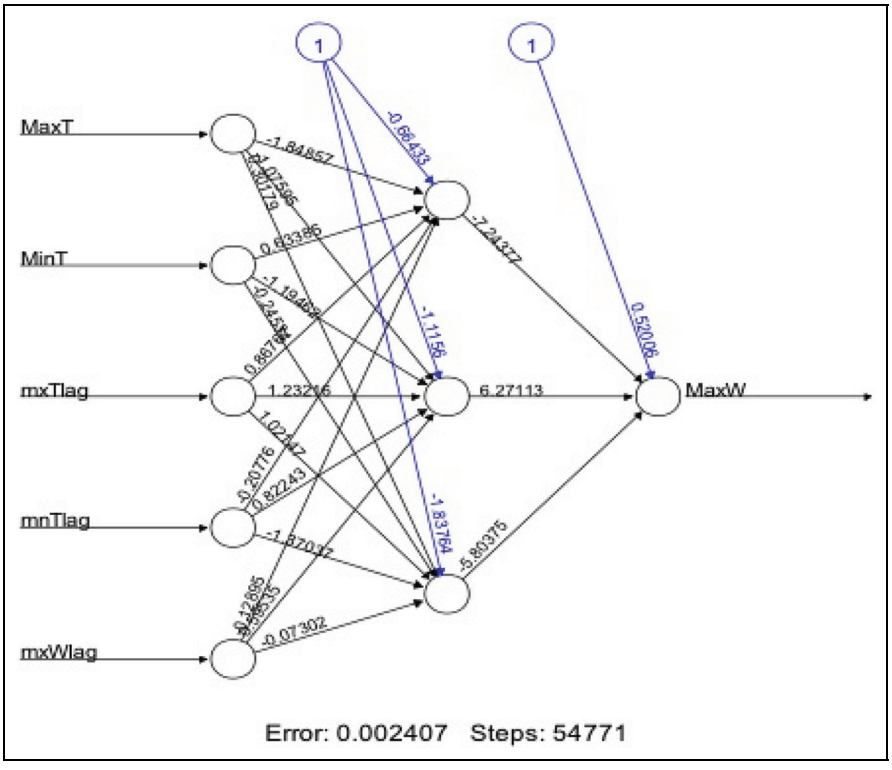

Figure 8. Plot of the artificial neural network showing three neurons in one hidden layer with input and output layers.

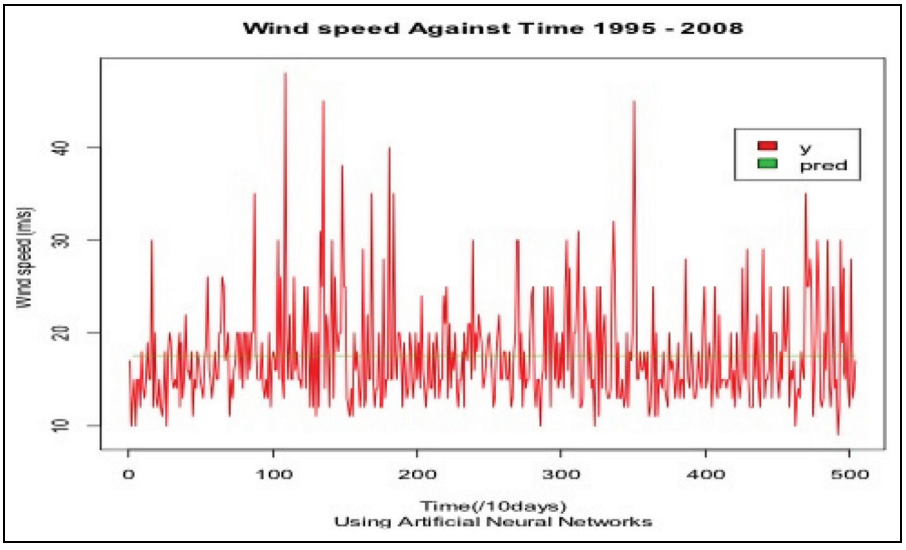

Figure 9. Plot of original wind speed and the artificial neural network model prediction.

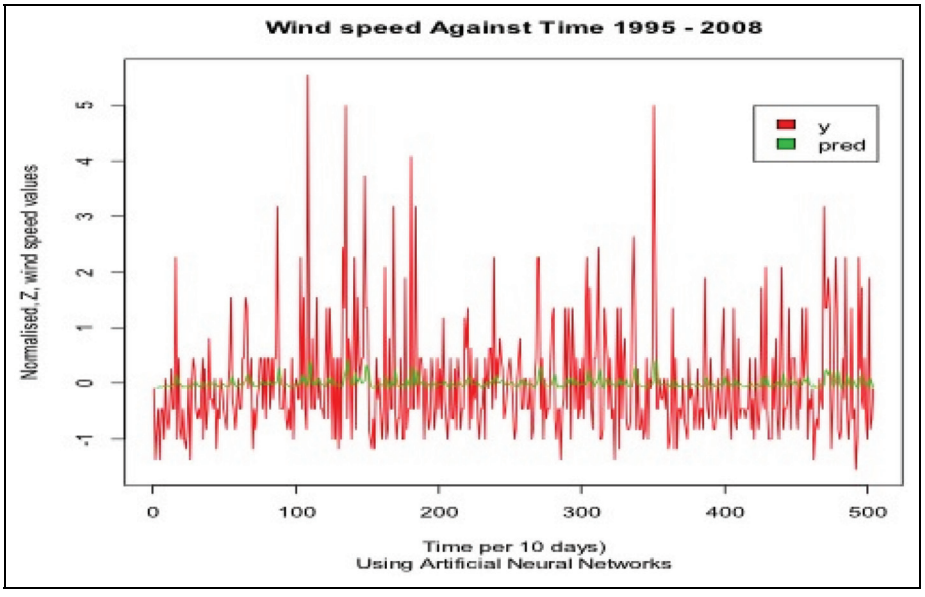

Figure 10. Plot of normalized original wind speed and the artificial neural network model prediction.

even better because of the smaller residuals, most of which cancel at zero.

The ANN, like the ARIMA model, predicted an average wind maximum speed of approximately 17.524 m/s. Figure 9 shows a plot of the original maximum wind series and the predicted values. The model presupposes that no matter the change in time and sometimes the large variations, the mean wind speed will approximately be the same in our case study.

A question of whether there are variations between standardized wind speeds was studied. As shown in Figure 10, the variations over the period were not significantly different from mean zero (0), but noises were observed over the series.

Further simulations with MATLAB's Neural Network Toolbox using the Levenberg–Marquardt training algorithm yielded optimal values at 10 hidden neurons and a delay of 2. The Neural Network Model training, validation, and testing results are presented in Table 3. Smaller values of the mean square error (MSE) are desirable because they indicate non-significant deviations from the actual data, hence a better model, while larger values of R (0.9) close to unity

Table 3. Results based on the MATLAB Neural Network Toolbox.

Neural network phase	Target values	Mean square error	*R*-value
Training	352	3.019e-8	0.9999
Validation	76	3.230e-8	0.9999
Testing	76	4.595e-8	0.9999

Table 4. Performance indices for the artificial neural network (ANN) and autoregressive integrated moving average (ARIMA) wind speed models.

Stochastic model	ME	RMSE	MAE	MPE	MAPE
ANN model	0.0025	0.0917	0.0380	− 0.0008	0.1845
ARIMA model	− 0.2252	5.4963	4.0393	6.3597	22.9031

ME: mean error; RMSE: root mean square error; MAE: mean absolute error; MPE: mean percentage error; MAPE: mean absolute percentage error.

imply a strong positive correlation between the original wind speed and that predicted by the derived neural network model.

Forecast errors were examined to evaluate the performance of the ANN and ARIMA prediction models using performance indices, as shown in Table 4.

Table 4 shows a comparison of performance indices for the ANN and ARIMA models using wind speed at an international airport. With the observed smaller values derived from the errors of estimation, it is clear that the ANN forecast model for the wind speed outperformed the ARIMA model under all the performance indices considered. For example, whereas the MAPE under the ANN model was 0.19%, it was 22.9% under the ARIMA model framework, implying that the forecast inaccuracy was higher in the later prediction model. A practical significance of these results is that to provide more accurate predictions of the usually intermittent and often-unstable characteristic of wind speed, the ANN model framework would be more useful than the ARIMA model framework.

Table 5. Descriptive statistics for residuals of prediction for the artificial neural network (ANN) and autoregressive integrated moving average (ARIMA) models.

Statistic	ANN model	ARIMA model
Mean wind speed	0.0026	0.2255
Standard error	0.0041	0.2449
Median	− 0.0063	− 0.8764
Standard deviation	0.0916	5.4972
Sample variance	0.0084	30.2197
Kurtosis	79.2930	4.4184
Skewness	7.6514	1.6496
Range	1.3322	39.6758
Minimum	− 0.1658	− 8.8486
Maximum	1.1664	30.8272
Sum	1.3110	113.6454
Count	504	504
Confidence level (95%)	0.0080	0.4811

4. Discussion

The ANN and ARIMA models were found to provide competitive model frameworks for the prediction of decadal wind speed. The ARIMA model was evaluated resulting in the ARIMA (0, 1, 1) model, implying a differencing and MA of 1 and 1, respectively. The ANN model fitted better with a single hidden layer of three neurons than one with five neurons. Using the AIC and the BIC for ARIMA and ANN model evaluations generated $AIC = 3149.78$; $BIC = 3158.22$ and $AIC = 72.01; BIC = 224.02$, respectively. Analysis of residuals for the ARIMA and ANN models using mean residuals showed a considerable difference between ARIMA (0.2255) and ANN (0.0026), as shown in Table 5.

Furthermore, forecast errors were plotted. Figure 11 shows a plot of the histogram with an approximate normal distribution curve bearing more clustering between forecast errors for the ANN than the ARIMA model framework, indicating further that the ANN model performed considerably better than the ARIMA model[36] due to a lower bound exhibited on the error of estimation.

In this study, stochastic models have been explored to predict wind speed time series data. ARIMA and ANN models were developed and predictions derived for wind speed data. Using a dataset of wind speed and related covariates for the period 1995–2008 at Entebbe International Airport, the models' efficacies were tested and evaluated and predictions made. An assessment of model residuals for both frameworks within the period of the study was comprehensively done through simulations and AIC and BIC computations were used to compare their efficiencies

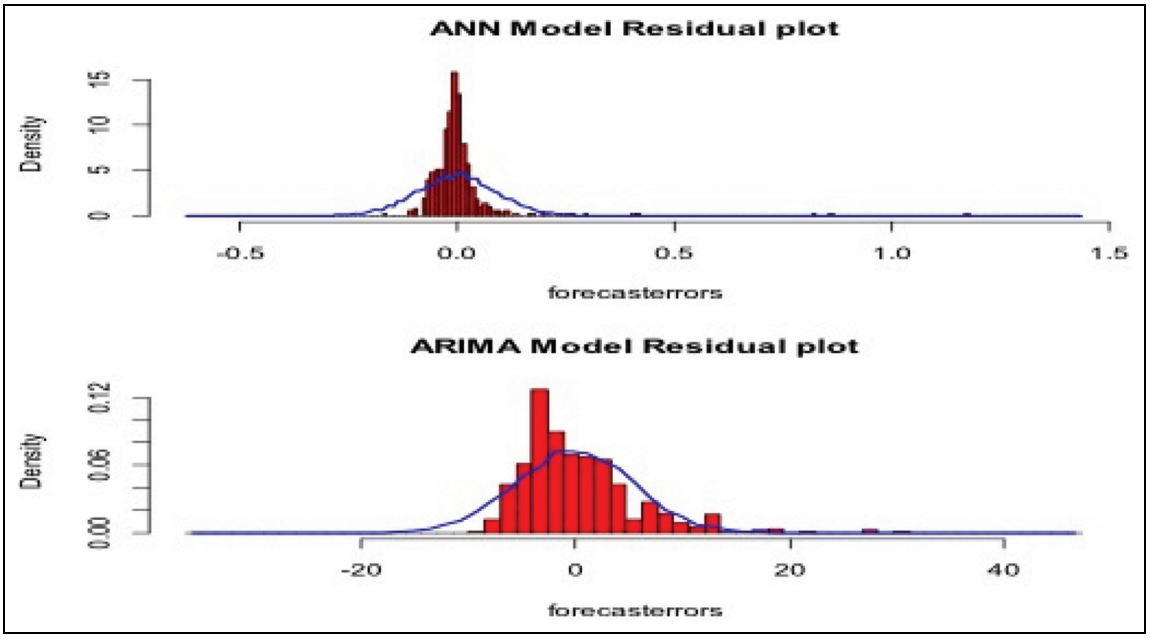

Figure 11. Artificial neural network (ANN) and autoregressive integrated moving average (ARIMA) model residual plots.

and prediction performances. The ANN model was evaluated using both linear and nonlinear conditions for the given inputs with different numbers of neurons in the hidden layers to derive a model for the ANN.[37–39] The ARIMA model was evaluated with different levels for *p, d*, and *q* values to derive the best model for the given type of data. However, due to the influence of sporadic wind speed data in the case study, the ARIMA (*p, d, q*) model simply reduced to a MA model framework.

5. Conclusions

Our study has shown that whereas wind speeds at Entebbe International Airport are a key impediment to the smooth flow of air traffic, they are also a great resource to the generation of power for the sustenance of clean energy at this airport. The case of decadal wind speed data modeling reveals a consistent and largely predictable high wind speed phenomenon. The ANN framework delivered smaller residuals, AIC, and BIC compared to the ARIMA model framework. The performance, indices including the MAE, MAPE, RMSE, mean error (ME), and mean percentage error (MPE), further confirmed the superiority of the ANN model over the ARIMA model. The study adds to the body of knowledge about the efficiency of models in time series prediction. Additional improvements to the ANN model are possible by accommodating fewer hidden layers with more hidden nodes. The wind speed prediction accuracy can be improved to secure the safety of air traffic flow as well support the implementation of a reliable and secure power generation system at the airport.

Funding

This research received no specific grant from any funding agency in the public, commercial, or not-for-profit sectors.

ORCID iD

Ronald Wesonga https://orcid.org/0000-0003-4887-9088

References

1. Barrett JE. Information-adaptive clinical trials: a selective recruitment design. *J R Stat Soc Ser C Appl Stat* 2016; 65: 797–808.
2. El-Shafie A. Neural network nonlinear modeling for hydrogen production using anaerobic fermentation. *Neur Comput Appl* 2014; 24: 539–547.
3. Jha G and Sinha K. Time-delay neural networks for time series prediction: an application to the monthly wholesale price of oilseeds in India. *Neur Comput Appl* 2014; 24: 563–571.
4. Ferreira AG, Soria-Olivas E, Lopez AJS, et al. Estimating net radiation at surface using artificial neural networks: a new approach. *Theor Appl Climatol* 2011; 106: 263–279.
5. de Oliveira M. The influence of ARIMA-GARCH parameters in feed forward neural networks prediction. *Neur Comput Appl* 2011; 20: 687–701.
6. Durdu O and Faruk. Application of linear stochastic models for drought forecasting in the B-Menderes river basin, western Turkey. *Stochast Environ Res Risk Assess* 2010; 24: 1145–1162.
7. Yusof F and Kane I. Volatility modeling of rainfall time series. *Theor Appl Climatol* 2013; 113: 247–258.

8. Wesonga R. Airport utility stochastic optimization models for air traffic flow management. *Eur J Oper Res* 2015; 242: 999–1007.
9. Wesonga R, Nabugoomu F and Jehopio P. Parameterized framework for the analysis of probabilities of aircraft delay at an airport. *J Air Transp Manag* 2012; 23: 1–4.
10. Verburg P and Hecky RE. Wind patterns, evaporation, and related physical variables in Lake Tanganyika, East Africa. *J Great Lakes Res* 2003; 29, Supplement 2: 48–61.
11. Latif M and Keenlyside NS. A perspective on decadal climate variability and predictability. *Deep Sea Res II Topical Stud Oceanogr* 2011; 58: 1880–1894.
12. Kirchner-Bossi N, Prieto L, Garca-Herrera R, et al. Multidecadal variability in a centennial reconstruction of daily wind. *Appl Energ* 2013; 105: 30–46.
13. Palomares-Salas JC, De la Rosa JJG, Ramiro JG, et al. ARIMA vs. neural networks for wind speed forecasting. In: *IEEE international conference on computational intelligence for measurement systems and applications, 2009 (CIMSA'09)*, Hong Kong, 11–13 May 2009, pp.129–133. Piscataway, NJ: IEEE.
14. Azad HB, Mekhilef S and Ganapathy VG. Long-term wind speed forecasting and general pattern recognition using neural networks. *IEEE Trans Sustain Energ* 2014; 5: 546–553.
15. Wesonga R. On multivariate imputation and forecasting of decadal wind speed missing data. *SpringerPlus*. 2015; 4: 4–12.
16. R Core Team. *R: a language and environment for statistical computing*. Vienna: R Foundation for Statistical Computing, 2014.
17. Avril C. *A little book of r for time series*. Cambridge: Parasite Genomics Group WTSI, 2014.
18. Soffritti G and Galimberti G. Multivariate linear regression with non-normal errors: a solution based on mixture models. *Stat Comput* 2011; 21: 523–536.
19. Box GEP, Jenkins GM and Reinsel GC. *Time series analysis: forecasting and control*. Hoboken, NJ: John Wiley & Sons, 2011.
20. Liang F. Bayesian neural networks for nonlinear time series forecasting. *Stat Comput* 2005; 15: 13–29.
21. Kisi O, Kim S and Shiri J. Estimation of dew point temperature using neuro-fuzzy and neural network techniques. *Theor Appl Climatol* 2013; 114: 365–373.
22. Bator R and Sieniutycz S. Application of artificial neural network for emission prediction of dust pollutants. *Int J Energ Res* 2006; 30: 1023–1036.
23. Mohandes MA, Rehman S and Halawani TO. A neural networks approach for wind speed prediction. *Renew Energ* 1998; 13: 345–354.
24. Kasiviswanathan KS and Sudheer KP. Quantification of the predictive uncertainty of artificial neural network based river flow forecast models. *Stochast Environ Res Risk Assess* 2013; 27: 137–146.
25. Jeong DI, St-Hilaire A, Ouarda TBMJ, et al. Comparison of transfer functions in statistical downscaling models for daily temperature and precipitation over Canada. *Stochast Environ Res Risk Assess* 2012; 26: 633–653.
26. Goyal MK. Monthly rainfall prediction using wavelet regression and neural network: an analysis of 1901–2002 data, Assam, India. *Theor Appl Climatol* 2014; 118: 25–34.
27. Goubanova K, Echevin V, Dewitte B, et al. Statistical downscaling of sea-surface wind over the Peru-Chile upwelling region: diagnosing the impact of climate change from the IPSL-CM4 model. *Clim Dynam* 2011; 36: 1365–1378.
28. Ghorbani MA, Khatibi R, Hosseini B, et al. Relative importance of parameters affecting wind speed prediction using artificial neural networks. *Theor Appl Climatol* 2013; 114: 107–114.
29. Yalcintas M and Akkurt S. Artificial neural networks applications in building energy predictions and a case study for tropical climates. *Int J Energ Res* 2005; 29: 891–901.
30. Ghanbarzadeh A, Noghrehabadi AR, Behrang MA, et al. Wind speed prediction based on simple meteorological data using artificial neural network. In: *7th IEEE international conference on industrial informatics, 2009 (INDIN 2009)*, Cardiff, 23–26 June 2009, pp.664–667. Piscataway, NJ: IEEE.
31. Aksoy H and Dahamsheh A. Artificial neural network models for forecasting monthly precipitation in Jordan. *Stochast Environ Res Risk Assess* 2009; 23: 917–931.
32. Aghajanloo M-B, Sabziparvar A-A and Hosseinzadeh Talaee P. Artificial neural network-genetic algorithm for estimation of crop evapotranspiration in a semi-arid region of Iran. *Neur Comput Appl* 2013; 23: 1387–1393.
33. Aziz K, Rahman A, Fang G, et al. Application of artificial neural networks in regional flood frequency analysis: a case study for Australia. *Stochast Environ Res Risk Assess* 2014; 28: 541–554.
34. Sivaram M. Modeling the price of trends of teak wood using statistical and artificial neural network techniques. *Electron J Appl Stat Anal* 2014; 7: 180–198.
35. Rehman S and Mohandes M. Estimation of diffuse fraction of global solar radiation using artificial neural networks. *Energ Sour A* 2009; 31: 974–984.
36. Sertelt E, Cigizoglu HK and Sanli DU. Estimating daily mean sea level heights using artificial neural networks. *J Coast Res* 2008; 24: 727–734.
37. Feijoo A, Villanueva D, Pazos JL, et al. Simulation of correlated wind speeds: a review. *Renew Sustain Energ Rev* 2011; 15: 2826–2832.
38. Petković D, Shamshirband S, Anuar N, et al. Adaptive neuro-fuzzy evaluation of wind farm power production as function of wind speed and direction. *Stochast Environ Res Risk Assess* 2015; 29: 793–802.
39. Guoqiang ZB, Eddy P and My H. Forecasting with artificial neural networks: the state of the art. *Int J Forecast* 1998; 14: 35–62.

Author biographies

Ronald Wesonga is an Assistant Professor at the Department of Mathematics and Statistics, Sultan Qaboos University, Muscat, Sultanate of Oman, and was a Senior Lecturer at the School of Statistics and Planning, Makerere University, Kampala, Uganda.

Fabian Nabugoomu is an Associate Professor and Deputy Vice Chancellor, Finance and Administration, at Kyambogo University, Kampala, Uganda.

Faisal Ababneh is an Assistant Professor at the Department of Mathematics and Statistics, Sultan Qaboos University, Muscat, Sultanate of Oman, and was an Associate Professor at Al-Hussein Bin Talal University Maan, Jordan.

Abraham Owino is a Senior Lecturer at the School of Statistics and Planning, Makerere University, Kampala, Uganda, and Director of the East African Statistics Institute.